Langmuir

Article

pubs.acs.org/Langmuir

# Amplification of Salt-Induced Polymer Diffusiophoresis by Increasing Salting-Out Strength

Michele S. McAfee,[†] Huixiang Zhang,[†,‡] and Onofrio Annunziata*

Contribution from the Department of Chemistry, Texas Christian University, Fort Worth, Texas 76129, United States

Supporting Information

**ABSTRACT:** The role of salting-out strength on (1) polymer diffusiophoresis from high to low salt concentration, and (2) salt osmotic diffusion from high to low polymer concentration was investigated. These two cross-diffusion phenomena were experimentally characterized by Rayleigh interferometry at 25 °C. Specifically, we report ternary diffusion coefficients for polyethylene glycol (molecular weight, 20 kg·mol$^{-1}$) in aqueous solutions of several salts (NaCl, KCl, $NH_4Cl$, $CaCl_2$, and $Na_2SO_4$) as a function of salt concentration at low polymer concentration (0.5% w/w). We also measured polymer diffusion coefficients by dynamic light scattering in order to discuss the interpretation of these transport coefficients in the presence of cross-diffusion effects. Our cross-diffusion results, primarily those on salt osmotic diffusion, were utilized to extract $N_w$, the number of water molecules in thermodynamic excess around a macromolecule. This preferential-hydration parameter characterizes the salting-out strength of the employed salt. For chloride salts, changing cation has a small effect on $N_w$. However, replacing NaCl with $Na_2SO_4$ (i.e., changing anion) leads to a 3-fold increase in $N_w$, in agreement with cation and anion Hofmeister series. Theoretical arguments show that polymer diffusiophoresis is directly proportional to the difference $N_w - n_w$, where $n_w$ is the number of water molecules transported by the migrating macromolecule. Interestingly, the experimental ratio, $n_w/N_w$, was found to be approximately the same for all investigated salts. Thus, the magnitude of polymer diffusiophoresis is also proportional to salting-out strength as described by $N_w$. A basic hydrodynamic model was examined in order to gain physical insight on the role of $n_w$ in particle diffusiophoresis and explain the observed invariance of $n_w/N_w$. Finally, we consider a steady-state diffusion problem to show that concentration gradients of strong salting-out agents such as $Na_2SO_4$ can produce large amplifications and depletions of macromolecule concentration. These effects may be exploited in self-assembly and adsorption processes.

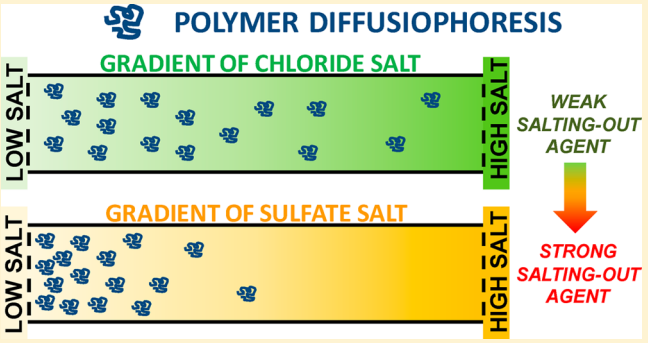


## 1. INTRODUCTION

Diffusion-based transport in multicomponent liquid systems[1−3] is important in separation science,[4] phase transitions,[5] adsorption on surfaces,[6] controlled-release technologies,[7] living-system dynamics,[8] reaction kinetics,[9] and pattern formation.[10] Diffusion becomes the dominant transport process in systems in which convection is absent as in the case of gels,[11,12] microfluidics[13−16] and near surfaces.[6,16] One not-well understood aspect of diffusion in multicomponent systems is the mechanism of cross-diffusion, i.e. diffusion of a solute due to the concentration gradient of another solute.[1−3,17,18] For colloidal particles under concentration gradients of additives, this mechanism is also known as diffusiophoresis.[19,20] Related experiments based on microfluidic devices have shown that differences in salt concentration produce significant migration of colloidal particles, thereby suggesting that salt concentration gradients with tunable amplitude and direction can cause strong particle diffusiophoresis leading to spreading or focusing of particles within the colloidal suspension.[21,22]

Nearly all studies on salt-induced diffusiophoresis have been limited to the case of large (≈100 nm) particles, in the presence of aqueous monovalent chloride salts (e.g., NaCl and KCl) at low salt concentration (≈0.1 mol·dm$^{-3}$ or less).[23,24] Since these particles are electrically charged, salt-induced diffusiophoresis at low ionic strengths has been satisfactorily described as the electrophoretic migration induced by a gradient of electric potential, emerging from the difference in mobility between counterion and co-ion of the salt component.[21,23,25]

Recently, we have shown that diffusiophoresis can be also observed in the case of macromolecules such as proteins and polymers.[26,27] In a first study, we have characterized protein diffusiophoresis for lysozyme in the presence of aqueous NaCl.[26] As in the case of colloidal particles, diffusiophoresis at low salt concentrations can be also described as an electrophoretic migration. However, at relatively high salt concentrations (>0.2 mol·dm$^{-3}$), hydration effects become increasingly more important and will significantly contribute to the magnitude of diffusiophoresis. In addition to protein

Received: August 13, 2014
Revised: September 16, 2014
Published: September 22, 2014

   dx.doi.org/10.1021/la503214b | Langmuir 2014, 30, 12210−12219

diffusiophoresis, we have also characterized salt diffusion induced by protein concentration gradients. This second cross-diffusion mechanism, denoted as salt osmotic diffusion, is directly related to preferential-hydration parameters,[28,29] describing protein-salt thermodynamic interactions in water. In a second study, we have characterized polymer diffusiophoresis and salt osmotic diffusion for polyethylene glycol (PEG) in the presence of aqueous KCl.[27] The choice of PEG was motivated by the following three aspects: (1) PEG is one of the most employed biocompatible synthetic macromolecule for pharmaceutical and industrial applications;[12,30,31] (2) it is a hydrophilic neutral polymer and hydration effects become the dominant source of salt-induced polymer diffusiophoresis;[27,32] and (3) it is available at several molecular weights. The last aspect has allowed us to experimentally show that the relative importance of diffusiophoresis compared to polymer intrinsic Brownian diffusion increases with polymer size.[27]

Since hydration effects drive salt-induced diffusiophoresis of PEG, it is important to know how this transport process depends on the chemical nature of the salt. Indeed, the role of salt type on the thermodynamic properties of macromolecular aqueous solutions has been extensively investigated.[33−37] In many studies, inorganic anions and cations have been ranked according to their salting-out strength, i.e., their effectiveness in precipitating proteins and synthetic polymers, leading to the well-known Hofmeister series.[38] In the case of anions, $SO_4^{2-}$ displays a great salting-out strength, while $Cl^-$ is regarded as neutral anion approximately located at the midpoint of the Hofmeister series, separating salting-out anions from salting-in anions, i.e., those increasing macromolecule solubility (e.g., $SCN^-$). Compared to anions, the Hofmeister series for cations is significantly less pronounced, and cation ranking may depend on the chemical nature of the investigated macromolecule. The most common cations, $Na^+$ and $K^+$, possess salting-out properties. Another familiar cation, $NH_4^+$, is usually positioned at greater salting-out strengths, though several studies have also shown that $NH_4^+$ display a salting-out strength weaker than those of both $Na^+$ and $K^+$. Common divalent cations, such as $Ca^{2+}$ and $Mg^{2+}$, are positioned at weaker salting-out strengths compared to alkali metal cations, and may display salting-in behavior depending on the chemical nature of the macromolecule.[36−38]

Our main goal is to characterize the effect salting-out strength of salts on the magnitude of salt-induced polymer diffusiophoresis. Specifically, precision Rayleigh interferometry[39] was used to determine the four ternary diffusion coefficients in aqueous solutions of PEG (molecular weight, 20 kg mol$^{-1}$) in the presence of NaCl, $NH_4Cl$, $CaCl_2$, and $Na_2SO_4$ at 25 °C. To our knowledge, diffusiophoresis studies with strong salting-out agents such as sulfate salts have not been reported yet. Our results are examined together with those previously reported for KCl.[32]

For ternary polymer(1)−salt(2)−water(0) systems, the extended Fick's first law is[3,27]

$$-\begin{bmatrix} J_1 \\ J_2 \end{bmatrix} = \begin{bmatrix} D_{11} & D_{12} \\ D_{21} & D_{22} \end{bmatrix} \times \begin{bmatrix} \nabla C_1 \\ \nabla C_2 \end{bmatrix} \quad (1)$$

where $C_1$ and $C_2$ are the molar concentrations of polymer and salt respectively, $J_1$ and $J_2$ are the corresponding molar fluxes, and the $D_{ij}$'s (with $i,j$ = 1,2) are the four multicomponent diffusion coefficients. Main-diffusion coefficients, $D_{11}$ and $D_{22}$, describe the flux of polymer and salt due to their own concentration gradients, while cross-diffusion coefficients, $D_{12}$ and $D_{21}$, which describe the flux of a solute due to the concentration gradient of the other solute, represent polymer diffusiophoresis and salt osmotic diffusion, respectively.[26,27]

In relation to these ternary systems, we also observe that polymer diffusion coefficients have been commonly determined by dynamic light scattering (DLS).[40] Since salt diffusion cannot be detected by DLS, the polymer diffusion coefficient is the only parameter that can be extracted from this technique.[39] Furthermore, contrary to Rayleigh interferometry, in which macroscopic gradients of solute concentrations can be varied by performing different experiments, DLS probes the effects of gradients associated with spontaneous microscopic fluctuations of solute concentrations. This ultimately leads to the conclusion that the DLS diffusion coefficient, $D_{DLS}$, does not coincide with $D_{11}$ but with the lower eigenvalue of the 2 × 2 $D_{ij}$ matrix.[39,41] To examine the effect of salting-out strength on the deviation of $D_{DLS}$ from the main-diffusion coefficient, $D_{11}$, we have also performed DLS experiments on these systems.

## 2. EXPERIMENTAL SECTION

**2.1. Materials.** PEG with nominal weights of 20 kg mol$^{-1}$ was purchased from Sigma-Aldrich and used without further purification. For PEG, certificates of analysis obtained from Sigma-Aldrich give the number ($M_n$) and mass average ($M_w$) molecular weights based on size-exclusion chromatography: $M_n$ =18.00 kg mol$^{-1}$ and $M_w/M_n$ =1.37. Stock concentrated solutions of PEG were made by weight to 0.1 mg. Density measurements (Mettler-Paar DMA40 density meter) were performed on the stock solutions for buoyancy corrections. Mallinckrodt AR KCl (purity, 99.9%; molecular weight, 74.55 g mol$^{-1}$) was dried by heating at 450 °C for 7 h and used without further purification.[42] Mallinckrodt AR NaCl (purity, 99.9%; molecular weight, 58.44 g mol$^{-1}$) was dried by heating at 400 °C for 4 h and used without further purification.[43,44] Fisher Scientific $NH_4Cl$ (A.C.S.; purity, ≥ 99.5%; molecular weight, 53.49 g mol$^{-1}$) was used without further purification. Sigma-Aldrich dihydrated $CaCl_2$ (ACS reagent plus; purity, ≥ 99.0%; molecular weight, 110.98 g mol$^{-1}$) was used, without further purification, to prepare $CaCl_2$-water stock solutions. The salt concentration of the stock solution was determined by measuring its density and using the available density-concentration relation.[44] Baker Analyzed ACS reagent (J.T. Baker) anhydrous $Na_2SO_4$ (purity, 99.7%; molecular weight, 142.04 g mol$^{-1}$) was used, without further purification, to prepare $Na_2SO_4$-water stock solutions. The salt concentration of the stock solution was determined by measuring its density and using the available density-concentration relation.[45,46] Deionized water was passed through a four-stage Millipore filter system to provide high-purity water for all the experiments. All solutions were prepared by mass. For binary PEG−water experiments, PEG stock solutions were diluted with pure water to reach the target PEG concentrations. For binary salt−water solutions, pure salt (KCl, NaCl, $NH_4Cl$) or concentrated salt-water stock solutions ($CaCl_2$, $Na_2SO_4$) were added to flasks and diluted with pure water to reach the target salt concentrations. For ternary PEG-salt-water solutions, PEG stock solution and salt (pure or stock solution) were added to flasks and diluted with pure water to reach the target PEG and KCl concentrations. Solution densities were measured to determine partial molar volumes and molar concentrations of polymer ($C_1$, based on the molecular weight of 20 kg mol$^{-1}$) and salt ($C_2$).

**2.2. Rayleigh Interferometry.** Binary and ternary mutual diffusion coefficients were measured at 25.00 ± 0.01 °C with the Gosting Diffusiometer operating in the Rayleigh interferometric optical mode.[47] The refractive-index profile inside a diffusion cell is measured as described in ref 39 and references therein. This yields diffusion coefficients in the volume-fixed reference frame.[47,48] The ternary diffusion coefficients, $D_{ij}$, were obtained by applying the method of the nonlinear least-squares to the refractive-index profiles as


dx.doi.org/10.1021/la503214b | Langmuir 2014, 30, 12210−12219

described in ref 49. Due to PEG molecular-weight polydispersity, a corrective procedure[50] based on the experimental refractive-index profiles of binary PEG−water systems was applied to our ternary experiments in order to remove the contribution of polydispersity from the ternary refractive-index profiles.

**2.3. Dynamic Light Scattering.** Diffusion measurements by DLS were performed at 25.0 ± 0.1 °C on binary PEG−water and ternary PEG−salt−water solutions. All samples were filtered through a 0.02-$\mu$m filter (Anotop 10, Whatman). The experiments were performed on a light-scattering apparatus built using the following main components: He−Ne laser (35 mW, 632.8 nm, Coherent Radiation), manual goniometer and thermostat (Photocor Instruments), multitau correlator, APD detector and software (PD4042, Precision Detectors). All experiments were performed at the scattering angle $\theta = 90°$; the value of the scattering vector $q = (4\pi n/\lambda) \sin(\theta/2)$ was calculated using $n = 1.33$ and $\lambda = 632.8$ nm. The scattered-intensity correlation functions were analyzed using a regularization algorithm (Precision Deconvolve 32, Precision Detectors).[51] All experimental correlation functions give monomodal diffusion-coefficient distributions. The DLS diffusion coefficient, $D_{DLS}$, was taken as the $z$-average diffusion coefficient of the obtained distributions.[40,50,51]

## 3. RESULTS AND DISCUSSION

Our experimental ternary diffusion coefficients determined in the volume-fixed reference frame are available as Supporting Information together with the corresponding diffusion coefficients in the solvent-fixed reference frame[3,48] and related volumetric properties. Values of $D_{ij}$ were obtained at the PEG concentration of $C_1 = 0.250 \times 10^{-3}$ mol·dm$^{-3}$ (5.00 g·dm$^{-3}$) as a function of salt concentration, $C_2$. In the following sections, we will first describe the behavior of polymer main-diffusion coefficients in relation to DLS and then examine our cross-diffusion results.

**3.1. Polymer Diffusion.** The behavior of $D_{11}$ as a function of salt concentration can be examined by first considering the effect of salt on solution viscosity as described by the Stokes-Einstein equation.[52] If this were the only factor shaping the salt-dependence of polymer diffusion, then $D_{11}$ would be equal to $D_1/\eta_2^r$, where $D_1$ is the value of PEG binary diffusion coefficient[27] at the same polymer concentration, and $\eta_2^r$ is the relative viscosity of the binary salt-water systems[53−55] at the same salt concentration. Thus, it is useful to calculate $D_{11}\eta_2^r/D_1$. The values of this quotient, which are reported in Table 1, show that $D_{11}\eta_2^r$ increases with salt concentration in all salt cases. For the three monovalent chloride salts, the observed increases are approximately the same. To compare these values of $D_{11}\eta_2^r/D_1$ with those obtained for in the $CaCl_2$ and $Na_2SO_4$ cases, we matched the same osmolar concentrations. For example, we can consider $C_2 = 0.50$ mol·dm$^{-3}$ for NaCl, KCl and $NH_4Cl$, and $C_2 = 0.33$ mol·dm$^{-3}$ for $CaCl_2$ and $Na_2SO_4$; both $C_2$ values correspond to the osmolar concentration of 1.0 mol·dm$^{-3}$. Here, an increase of ≈1.7% in $D_{11}\eta_2^r$ is observed in the case of the monovalent chloride salts. In the $CaCl_2$ case, the corresponding increase is not significantly higher (2.1%), while, in the $Na_2SO_4$ case, it is almost 4-fold higher (6.6%).

**Table 1. Normalized Polymer Diffusion Coefficients**

| | NaCl | | KCl | | $NH_4Cl$ | |
|---|---|---|---|---|---|---|
| $C_2$/mol dm$^{-3}$ | $D_{11}\eta_2^r/D_1$ | $\mathcal{D}_1\eta_2^r/D_1$ | $D_{11}\eta_2^r/D_1$ | $\mathcal{D}_1\eta_2^r/D_1$ | $D_{11}\eta_2^r/D_1$ | $\mathcal{D}_1\eta_2^r/D_1$ |
| 0.50 | 1.020 ± 0.002 | 1.003 ± 0.002 | 1.016 ± 0.002 | 1.001 ± 0.002 | 1.016 ± 0.003 | 1.008 ± 0.003 |
| 1.00 | 1.033 ± 0.002 | 1.001 ± 0.002 | 1.037 ± 0.002 | 1.007 ± 0.002 | 1.032 ± 0.006 | 1.017 ± 0.006 |
| 2.00 | 1.070 ± 0.002 | 1.009 ± 0.002 | 1.065 ± 0.003 | 1.009 ± 0.003 | 1.049 ± 0.006 | 1.021 ± 0.006 |
| | $CaCl_2$ | | $Na_2SO_4$ | | | |
| $C_2$/mol dm$^{-3}$ | $D_{11}\eta_2^r/D_1$ | $\mathcal{D}_1\eta_2^r/D_1$ | $D_{11}\eta_2^r/D_1$ | $\mathcal{D}_1\eta_2^r/D_1$ | | |
| 0.10 | 1.016 ± 0.003 | 1.012 ± 0.003 | 1.025 ± 0.002 | 0.997 ± 0.002 | | |
| 0.20 | 1.011 ± 0.002 | 1.004 ± 0.002 | 1.041 ± 0.003 | 0.987 ± 0.003 | | |
| 0.33 | 1.021 ± 0.002 | 1.007 ± 0.002 | 1.066 ± 0.002 | 0.973 ± 0.002 | | |

The behavior of polymer diffusion in aqueous salt solutions was then characterized by DLS. This is a versatile technique that has the advantage of being more convenient compared to Rayleigh interferometry in terms of sample amounts, experimental execution, and measurement time, but it typically yields results at lower precision than interferometric methods.[39] The DLS diffusion parameter, $D_{DLS}$, is not the same as $D_{11}$ but it should be equal to the lower eigenvalue, $\mathcal{D}_1$, of the $D_{ij}$ matrix.[39,41] The condition $\mathcal{D}_{11} = \mathcal{D}_1$ applies when one of the two cross-diffusion coefficients is zero. This circumstance occurs in the limit of zero salt concentration, i.e., in the case of binary polymer−water systems, and in the limit of zero polymer concentration.[39] This implies that $D_{DLS}$ should coincide with the binary diffusion coefficient, $D_1(C_1)$, in the former case, and the tracer-diffusion coefficient, $D_1^0(C_2)$, in the latter case. However, instrumental bias[39] and polymer polydispersity[50] lead to systematic differences of ≈3% between DLS and Rayleigh interferometry in these two limiting cases. Since this discrepancy can be entirely attributed to an offset between the two values of $D_1^0$ extracted by DLS and Rayleigh interferometry, respectively, a reliable comparison between these two techniques can be performed after normalizing the measured diffusion coefficients with respect to the corresponding $D_1^0$ values.

DLS diffusion coefficients were measured for the binary PEG−water system and ternary PEG−salt−water systems as a function of PEG concentration (data available as Supporting Information). For the ternary systems, $C_2$ was kept constant at 1.0 mol·dm$^{-3}$ for NaCl, KCl, and $NH_4Cl$, and at 0.33 mol·dm$^{-3}$ for $CaCl_2$ and $Na_2SO_4$. In Figure 1A, we show $D_{DLS}\eta_2^r$ as a function of polymer volume fraction, $\phi_1 = C_1\bar{V}_1$, where $\bar{V}_1 = 16.7$ dm$^3$ mol$^{-1}$ (specific volume, 0.835 cm$^3$g$^{-1}$) is the partial molar volume of the investigated PEG,[27,32] which can be assumed to be constant within the experimental domain. For the binary system, linear extrapolation to $\phi_1 = 0$ yields $D_1^0 = 0.0552 \times 10^{-9}$ m$^2$ · s$^{-1}$. This value is 3.0% lower than that[27] obtained by interferometry.

For ternary systems, all linear extrapolations of $D_{DLS}\eta_2^r$ are in good agreement with the binary value within the experimental error (see Figure 1A). Hence, the dependence of $D_1^0$ on salt concentration can be entirely attributed to viscosity; i.e., $D_1^0(C_2) = D_1^0(0)/\eta_2^r(C_2)$. For the binary PEG−water system, $D_{DLS}$ increases with polymer concentration, consistent with previous studies.[27,32,56,57] Interestingly, the addition of chloride salts does not have a significant impact on the dependence of $D_{DLS}\eta_2^r$ on $\phi_1$, while that of $Na_2SO_4$ appreciably decreases the slope of $D_{DLS}\eta_2^r$ in Figure 1A. This implies that the effect of $Na_2SO_4$ concentration on $D_{DLS}\eta_2^r$ is the opposite of that observed in the case of $D_{11}\eta_2^r$. These two contrasting behaviors are illustrated in Figure 1B, where we can see that the binary $D_1/D_1^0$ and $D_{DLS}/D_1^0$ overlap within the experimental error while the normalized ternary diffusion coefficient for $Na_2SO_4$ at $C_2 = 0.33$ mol·dm$^{-3}$, $D_{11}/D_1^0$, is located above the binary line, and the ternary DLS data are on the opposite side. For comparison, we have also


dx.doi.org/10.1021/la503214b | Langmuir 2014, 30, 12210−12219

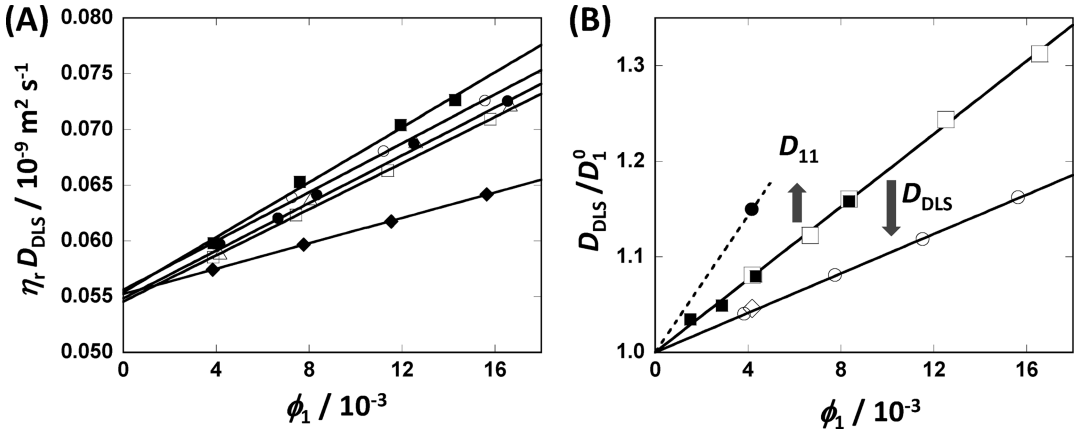


**Figure 1.** (A) Viscosity-corrected DLS diffusion coefficients, $D_{DLS}\eta_2^r$, as a function of PEG volume fraction, $\phi_1$, for the binary PEG−water system (solid circles), and the investigated ternary PEG−salt−water systems (NaCl, 1.0 mol dm$^{-3}$, open circles; 1.0 mol dm$^{-3}$ KCl, 1.0 mol dm$^{-3}$, open squares; $NH_4Cl$, 1.0 mol dm$^{-3}$, open triangles; $CaCl_2$, 0.33 mol dm$^{-3}$, solid squares; $Na_2SO_4$, 0.33 mol dm$^{-3}$, solid diamonds). The solid lines are linear fits through the data. (B) DLS diffusion coefficients, $D_{DLS}$, normalized with respect to the PEG tracer-diffusion coefficient, $D_1^0$, as a function of PEG volume fraction for the binary PEG−water system (open squares) and the ternary PEG−$Na_2SO_4$−water system (open circles). For comparison, normalized interferomentric diffusion coefficients for the binary PEG−water system (solid squares) taken from ref 27 are included together with the normalized main-diffusion coefficient, $D_{11}$ (solid circle), and the corresponding eigenvalue, $D_1$ (open diamond) related to $Na_2SO_4$, 0.33 mol dm$^{-3}$. The gray vertical arrows highlight the opposite effects of $Na_2SO_4$ on $D_{11}$ and $D_{DLS}$.

included the corresponding normalized eigenvalue, $\mathcal{D}_1/D_1^0$, where $D_1$ is given by the quadratic-equation root: $\mathcal{D}_1 = 0.5[(D_{11} + D_{22}) + (D_{11} - D_{22})(1 + x)^{1/2}$, with $D_{22} > D_{11}$ and $x \equiv 4D_{12}D_{21}/(D_{22} - D_{11})^2$. As we can see in Figure 1B, the value of $\mathcal{D}_1/D_1^0$ is in good agreement with the ternary DLS data, in agreement with DLS theory. For completeness, we report the $\mathcal{D}_1\eta_2^r/D_1$ values for all ternary diffusion data in Table 1. These are in agreement with DLS results in Figure 1A within the experimental error. Note that the behavior of $\mathcal{D}_1\eta_2^r/D_1$ observed in the $Na_2SO_4$ case ($\mathcal{D}_1\eta_2^r/D_1 < 1$), is the opposite of that observed in the case of chloride salts ($\mathcal{D}_1\eta_2^r/D_1 \gg 1$). This is related to cross-diffusion coefficients being relatively large in the $Na_2SO_4$ case, as it will be shown below.

The effect of cross-diffusion coefficients on the deviation of $\mathcal{D}_1$ from $D_{11}$ can be better appreciated by applying some inconsequential approximation. After examining the contribution of the four $D_{ij}$ in the eigenvalue expression of $\mathcal{D}_1$, we find that $x \ll 1$ for all our data. This is related to $D_{12}D_{21}$ being significantly smaller than $(D_{22})^2$, a condition that applies to macromolecule−salt systems because the mobility of salt ions is relatively high. Specifically, all values of $x$ were found to be less than 3.0%. This implies that the first-order series expansion $(1+x)^{0.5} \cong 1+0.5x$ is an excellent approximation; e.g., an error of 0.01% is obtained when $x = 0.03$. For instance, this approximation leads to the small error of 0.01% when $x = 0.03$. By applying this approximation, we obtain the following simple relation between $\mathcal{D}_1$ and cross-diffusion coefficients:

$$\mathcal{D}_1 \cong D_{11} - D_{12}D_{21}/(D_{22} - D_{11}) \tag{2}$$

Note that $\mathcal{D}_1$ is lower than $D_{11}$ because $D_{12}D_{21} > 0$ and $D_{22} > D_{11}$. Since $D_{12}$ and $D_{21}$ are directly proportional to $C_1$ and $C_2$, respectively,[58] and $D_{22} - D_{11} \approx D_{22}$ can be roughly regarded as constant, the difference between $D_{11}$ and $\mathcal{D}_1$ increases with polymer and salt concentrations.

**3.2. Cross-Diffusion Theory.** Cross-diffusion coefficients, $D_{12}$ and $D_{21}$, can be examined after appropriate normalizations. These are important because differences in salt stoichiometry (e.g., NaCl vs $Na_2SO_4$) and physical properties of binary salt−water systems (e.g., activity coefficients and diffusion coefficients) must be taken into account when comparing two different salt cases. Hence, the following two normalized cross-diffusion coefficients have been introduced:[27]

$$\hat{D}_{12} \equiv \lim_{C_1\to 0}[D_{12}/C_1 + \bar{V}_2D_2/(1 - C_2\bar{V}_2)]C_2/(\nu_2 y_2 D_1^0) \tag{3a}$$

$$\hat{D}_{21} \equiv \lim_{C_1\to 0}[D_{21} + C_2\bar{V}_1D_1^0]/D_2 \tag{3b}$$

where $D_2$, $\bar{V}_2$, and $y_2 \equiv 1 + d \ln y_\pm/d \ln C_2$, with $y_\pm$ being the salt mean-ionic activity coefficient, are salt diffusion coefficient (in volume-fixed frame), partial molar volume, and nonideality thermodynamic factor, respectively. The second term inside the square brackets of eqs 3a and 3b represents a correction needed to convert cross-diffusion coefficients from the volume- to the solvent-fixed frame.[27,48] Values of $D_2$ and $\bar{V}_2$ were extracted from our interferometric and density measurements respectively, while $y_2$ and $\eta_2^r$ values are literature data (see Supporting Information).[42,44−46,53−55] The coefficient $\nu_2$ in eq 3a describes electrolyte dissociation (e.g., $\nu_2 = 2$ for NaCl and $\nu_2 = 3$ $Na_2SO_4$). Values of $\hat{D}_{12}$ and $\hat{D}_{21}$ obtained at the same $C_2$ for two salts with different $\nu_2$ can be directly compared because they do not explicitly depend on the number of dissociating ions, $\nu_2$. Indeed, $D_{12}$ is divided by $\nu_2$ in eq 3a. This normalization is needed because $D_{12}$ is defined with respect to $\nabla C_2$ and not the corresponding osmolar-concentration gradient, $\nu_2\nabla C_2$. In other words, $D_{12}$ describes the effect of all ions on the polymer molar flux, $J_1$. On the other hand, $\nu_2$ does not appear in eq 3b because $D_{21}$ describes the effect of $\nabla C_1$ on the flux of the salt component, $J_2$, and not on the total flux of ions, $\nu_2 J_2$; i.e., $D_{21}$ is already independent of $\nu_2$.

According to irreversible thermodynamics, we can write[26,27]

$$\hat{D}_{12} = \gamma - \lambda \tag{4a}$$

$$\hat{D}_{21} = \gamma + C_2\bar{V}_1 - \alpha\lambda \tag{4b}$$

where $\gamma \equiv \lim_{C1\to 0}(\mu_{12}/\mu_{22})$ and $\lambda \equiv -\lim_{C1\to 0}(L_{12}/L_{11})$ are thermodynamic and transport quantities, respectively, $\mu_{ij} \equiv$


dx.doi.org/10.1021/la503214b | Langmuir 2014, 30, 12210−12219

$(\partial\mu_i/\partial C_j)_{Ck,k\neq j}$ are chemical-potential derivatives at constant temperature and pressure with $\mu_i$ being the chemical potential of component $i$, $L_{ij}$ are the Onsager transport coefficient in the solvent-fixed frame, and $\alpha \equiv D_1^0/D_2$. In eq 4b, the approximation $C_0\overline{V}_0 = 1-C_2\overline{V}_2 \approx 1$ has been used, where $C_0 \approx 1/\overline{V}_0$ is the water molar concentration, and $\overline{V}_0 = 18.07$ cm$^3$·mol$^{-1}$ is its molar volume. This approximation gives the maximum error of ≈5% when $C_2 \approx 2$ mol·dm$^{-3}$, an error that is comparable with that of cross-diffusion coefficients.

The thermodynamic quantity in eqs 4a and 4b can be written as $\gamma = N_w\ (C_2/C_0) \approx N_w\overline{V}_0C_2$, where $N_w$ is the thermodynamic excess of water molecules around a polymer coil according to preferential-interaction theory.[27−29] Its value characterizes the salting-out strength of the employed salt. On the other hand, the transport quantity in eqs 4a and 4b can be interpreted as $\lambda = n_w\ (C_2/C_0) \approx n_w\overline{V}_0C_2$, where $n_w$ is the number of water molecules transported by a polymer coil during diffusiophoresis.[26,27] Previous experimental studies[27] have shown that $n_w$ significantly contributes to diffusiophoresis. Hence, $\hat{D}_{12}$ cannot be approximately described as a thermodynamic quantity, i.e., we cannot write $\hat{D}_{12} \approx \gamma$ neglecting the contribution $\lambda$ in eq 4a. On the other hand, since $\alpha$ is small (see Supporting Information) and the magnitude of $\gamma$ is comparable to that of $\lambda$, the contribution of $\alpha\,\lambda$ in eq 4b is well below 10%; i.e., $\hat{D}_{12} \approx \gamma + C_2\overline{V}_1$ is approximately a thermodynamic quantity. Due to the marginal role of $\alpha$ and its weak dependence on salt concentration, it is an excellent approximation to assume that this parameter in eq 4b is a constant independent of salt concentration. For each salt, the corresponding average value of $\alpha$ is reported in Table 2.

**Table 2. Cross-Diffusion Parameters**

| | NaCl | KCl | $NH_4Cl$ | $CaCl_2$ | $Na_2SO_4$ |
|---|---|---|---|---|---|
| $\alpha$ | 0.035 | 0.030 | 0.029 | 0.045 | 0.053 |
| $b_{12}$/ mol$^{-1}$dm$^3$ | 2.51 ± 0.05 | 2.58 ± 0.02 | 1.83 ± 0.03 | 1.97 ± 0.10 | 7.42 ± 0.06 |
| $b_{21}$/ mol$^{-1}$dm$^3$ | 35.7 ± 0.1 | 34.5 ± 0.1 | 32.1 ± 0.3 | 34.3 ± 0.5 | 77.7 ± 0.7 |
| $N_w$ | 1090 | 1010 | 860 | 970 | 3540 |
| $N_w-n_w$ | 139 | 143 | 101 | 111 | 410 |
| $n_w/N_w$ | 0.872 | 0.859 | 0.882 | 0.886 | 0.884 |

From these theoretical considerations, we deduce that both $\hat{D}_{12}$ and $\hat{D}_{21}$ are directly proportional to $C_2$, provided that $N_w$ and $n_w$ can be regarded as independent of salt concentration. Furthermore, $\hat{D}_{12}$ is proportional to the volume difference: $(N_w - n_w)\overline{V}_0$, while $\hat{D}_{21}$ is proportional to the total volume: $N_w\overline{V}_0 + \overline{V}_1$, i.e., the volume of the local domain of a macromolecule, completely depleted of the salt component (excluded volume).

**3.3. Cross-Diffusion Experimental Results.** Since the experimental polymer concentration is fairly low, $D_{12}$ and $D_{21}$ values can be directly used to calculate $\hat{D}_{12}$ and $\hat{D}_{21}$ as a function of salt concentration, $C_2$, within the experimental error of cross-diffusion coefficients.[26,27] Consistent with the validity of this approximation, irreversible thermodynamics shows that the nonideality thermodynamic factor describing polymer−polymer interactions does not contribute to $D_{12}$ and has a negligible effect on $D_{21}$.[27] After converting $D_{12}$ and $D_{21}$ into the corresponding $\hat{D}_{12}$ and $\hat{D}_{21}$, we plot our results as a function of salt concentration in Figure 2A,B for NaCl, KCl, and $NH_4Cl$, and Figure 3A,B for $CaCl_2$ and $Na_2SO_4$. The baselines $\hat{D}_{21} = \overline{V}_1C_2$ (dotted lines), which correspond to $N_w = 0$ (with $\alpha \to 0$), are included in Figure 2B and Figure 3B for comparison. Both $\hat{D}_{12}$ and $\hat{D}_{21}$ are proportional to salt concentration and approach zero as $C_2 \to 0$, in agreement with theory. According to eq 4b, a positive deviation of $\hat{D}_{21}(C_2)$ from the dotted line, $\overline{V}_1\ C_2$, approximately quantifies the salting-out strength of the salt. In Figure 2B, we can see that the contribution of $N_w\overline{V}_0\ C_2$ to $\hat{D}_{21}$ is roughly the same as that of $\overline{V}_1C_2$, while it becomes about 3-fold larger for the $Na_2SO_4$ case in Figure 3B. Note that $\hat{D}_{21}(C_2)$ displays some curvature at salt concentrations higher than ≈1 mol ·dm$^{-3}$, a feature that we interpret as a corresponding reduction of $N_w$. This behavior may be related to the compression of polymer coils caused by salt-induced osmotic stress. The $\hat{D}_{12}(C_2)$ and $\hat{D}_{21}(C_2)$ curves for NaCl are approximately the same as those obtained for KCl, while the corresponding $NH_4Cl$ curves display an appreciably smaller slope.

Since the experimental range of salt concentrations in the $CaCl_2$ and $Na_2SO_4$ cases is significantly narrower than that in Figure 2A,B, the corresponding $\hat{D}_{12}(C_2)$ and $\hat{D}_{21}(C_2)$ curves are separately shown in Figure 3A,B. For comparison, dashed lines representing our results for NaCl are included. The obtained results for $CaCl_2$ are similar to those obtained for the other chloride salts, while those obtained for $Na_2SO_4$ show a significantly larger slope, consistent with the anion being more important than the cation in the relative ranking of salting-out strengths.

To quantify the magnitude of cross-diffusion, we apply the method of least-squares to our data based on the linear relations, $\hat{D}_{12} = b_{12}C_2$ and $\hat{D}_{21} = b_{21}C_2$, and determine $b_{12}$ and $b_{21}$. In the case of $\hat{D}_{21}$, we do not use data in Figure 3B with salt concentrations higher than ≈1 mol·dm$^{-3}$. In Table 2, we report the values of $b_{12}$ and $b_{21}$ together with the extracted hydration parameters, $N_w$ and $N_w - n_w$. In the case of all chloride salts (independent of salt stoichiometry), the observed water thermodynamic excess is $N_w \approx 1000$; this corresponds to ≈2 water molecules per PEG monomeric unit. The extracted values of $N_w$ for the four chloride salts are very close to each other, ranging from ≈900 for $NH_4Cl$ to ≈1100 for NaCl; they are consistent with the following ranking of cations: $Na^+ > K^+ > Ca^{2+} > NH_4^+$. While the position of the first three cations in our ranking agrees with the Hofmeister series,[36−38] that of the ammonium ion requires further comments. Since this ion is typically located at higher salting-out strengths, our results are in disagreement with the most common ranking given in literature. However, as mentioned in the introduction, the location of $NH_4^+$ may strongly depend on the chemical nature of investigated macromolecule.[36] This is related to the capability of this ion to form hydrogen bonds with macromolecules. In our case, we attribute the relatively weak salting-out strength of $NH_4^+$ to hydrogen bonding with the PEG oxygen atoms. Since a binding mechanism promotes the accumulation of salt ions around a macromolecule, this weak attractive interaction contributes negatively to a net value of $N_w$. A relatively weak salting-out strength of ammonium chloride was also observed in the case of the protein lysozyme[59]

To assess the effect of anion substitution on $N_w$, we compare NaCl to $Na_2SO_4$. For $Na_2SO_4$, the obtained $N_w$ value, which corresponds to an excess of 7.8 water molecules per PEG monomeric unit, was found to be considerably (3.2-fold) higher than that obtained for NaCl (see Table 2). This is consistent with the anion Hofmeister series, and shows the more important role played by the anions in the salting-out ranking of salts.[38]


dx.doi.org/10.1021/la503214b | Langmuir 2014, 30, 12210−12219

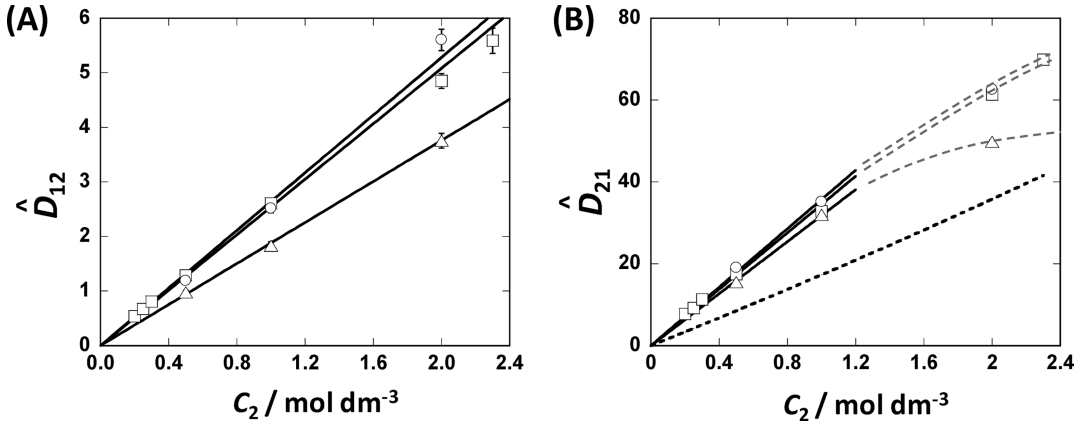


**Figure 2.** (A) Normalized cross-diffusion coefficients, $\hat{D}_{12}$, as a function of salt concentration, $C_2$, characterizing PEG diffusiophoresis in the presence of NaCl (circles), KCl (squares) and $NH_4Cl$ (triangles). The solid lines are one-parameter weighed linear fits through the data satisfying the relation $\hat{D}_{12} = b_{12}C_2$, with $\hat{D}_{12} = 0$ at $C_2 = 0$. (B) Normalized diffusion coefficients, $\hat{D}_{21}$, as a function of salt concentration, $C_2$, describe salt osmotic diffusion in the presence of NaCl (circles), KCl (squares), and $NH_4Cl$ (triangles). The solid lines are one-parameter linear fits through the data satisfying the relation $\hat{D}_{21} = b_{21}C_2$, with $\hat{D}_{12} = 0$ at $C_2 = 0$. The corresponding gray dashed extensions are eye guides showing data curvature at high salt concentrations. The dotted line is the graphical representation of $\hat{D}_{21} = \bar{V}_1C_2$.

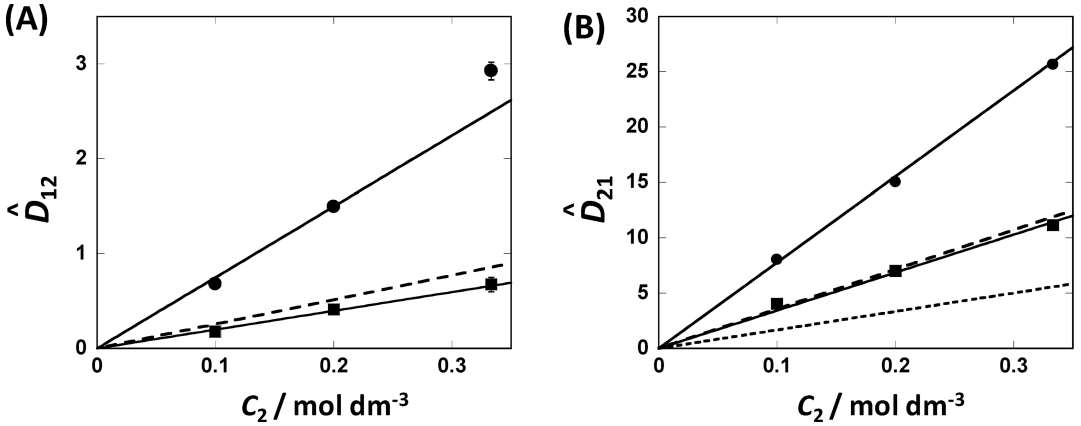


**Figure 3.** (A) Normalized diffusion coefficients, $\hat{D}_{12}$, as a function of salt concentration, $C_2$, describe PEG diffusiophoresis in the presence of $CaCl_2$ (squares) and $Na_2SO_4$ (circles). The solid lines are one-parameter weighed linear fits through the data satisfying the relation $\hat{D}_{12} = b_{12}C_2$, with $\hat{D}_{12} = 0$ at $C_2 = 0$. For comparison, $\hat{D}_{12} = b_{12}C_2$ for the NaCl case (dashed line) is included. (B) Normalized diffusion coefficients, $\hat{D}_{21}$, as a function of salt concentration, $C_2$, describe salt osmotic diffusion in the presence of $CaCl_2$ (squares) and $Na_2SO_4$ (circles). The solid lines are one-parameter linear fits through the data satisfying the relation $\hat{D}_{21} = b_{21}C_2$, with $\hat{D}_{21} = 0$ at $C_2 = 0$. For comparison, $\hat{D}_{21} = b_{21}C_2$ for the NaCl case (dashed line) is included. The dotted line is the graphical representation of $\hat{D}_{21} = \bar{V}_1C_2$.

We now turn our attention to the difference $N_w - n_w$, which characterizes the magnitude of polymer diffusiophoresis. The values of $N_w - n_w$ reported in Table 2 are one order of magnitude smaller than the corresponding values of $N_w$. This implies that the kinetic parameter, $n_w$, cannot be neglected compared to $N_w$. Nonetheless, the values of $N_w - n_w$ essentially follow the same trend shown for $N_w$. Specifically, the values obtained for the chloride salts are very close to each other, ranging from ≈100 for $NH_4Cl$ to ≈140 for NaCl and KCl, and are consistent with the following ranking of cations: $K^+ \approx Na^+ > Ca^{2+} > NH_4^+$. The value of $N_w - n_w$ for $Na_2SO_4$ was also found to be significantly (2.9-fold) higher than that obtained for NaCl. Thus, our experimental results show that, in addition to $N_w$, the difference $N_w - n_w$ can also be used to rank salts with respect to their salting-out strength. In other words, salt-induced polymer diffusiophoresis is directly proportional to the salting-out strength of the salt component. This conclusion can be explained by assuming that the ratio $n_w/N_w$ is independent of salting-out strength as indicated by the $n_w/N_w$ values in Table 2, where the $n_w/N_w$ value for $Na_2SO_4$ is within the range of those for the chloride salts, which fluctuate between 0.86 and 0.89.

**3.4. Hydrodynamic Model.** The observed behavior of $N_w - n_w$ cannot be straightforwardly deduced from that of $N_w$ because there is no theoretical relation between the kinetic parameter $n_w$ and salting-out strength. In order to gain some physical insight on the role that $n_w$ plays in diffusiophoresis under salting-out conditions, we have applied a hydrodynamic model to an idealized particle in the presence of the gradient of an additive, describing the role of salt. It is important to remark that the role of particle shape and specific chemical interactions will be ignored. Nonetheless, we believe that these factors are not crucial if we restrict our goals to a conceptual understanding of $n_w$ in diffusiophoresis and its connection to salting-out strength.

We consider a simple hydrodynamic model for particle diffusiophoresis induced by a constant gradient of additive concentration, $dC_2/dx$, along the $x$ direction. For simplicity, the particle is large enough that its interface with the surrounding fluid can be regarded as flat (see Figure 4). The hydrodynamic


dx.doi.org/10.1021/la503214b | Langmuir 2014, 30, 12210−12219

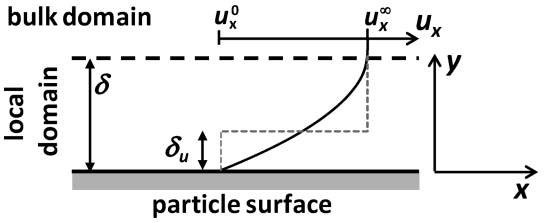


**Figure 4.** Diagram showing the profile of solvent velocity, $u_x$ (solid curve), parallel to the particle surface (solid horizontal line along the $x$ axis) as a function of the vertical distance from the particle, $y$, with $u_x = u_x^0 \equiv 0$ and $u_x = u_x^\infty$ at $y = 0$ and $y = \delta$, respectively. The horizontal dashed line at $y = \delta$ separates the local domain from the bulk domain. The position $y = \delta_u = \delta/3$ is chosen such that the net area between the gray dashed step function and the velocity profile, $u_x(y)$, is zero.

model that will be examined in this section has been already applied to diffusiophoresis.[19] However, to our knowledge, the significance of the solvation parameter, $n_w$, in diffusiophoresis has not yet been addressed.

The additive salting-out strength is described by the simple mean-force potential: $W = 0$ if $y \geq \delta$ and $W = \infty$ if $y < \delta$, where $y$ is the distance from the particle interface (see Figure 4), and $\delta$ is the thickness of the layer around the particle, within which the interaction with the additive occurs. This layer represents the local domain of the particle. Additive depletion near the particle interface is described by the additive concentration profile $G_2(x,y)$; it follows that $G_2(x,y > \delta) = C_2(x)$ and $G_2(x,y < \delta) = 0$ from the Boltzmann distribution: $G_2 = C_2 \exp(-W/k_BT)$, where $k_B$ is the Boltzmann constant and $T$ is the temperature. Since the additive is completely excluded from the local domain, the excess of solvent molecules is the total number of solvent molecules in the local domain:[29] i.e., $N_w = \sigma \delta/v_w$, where $v_w$ is the volume occupied by a solvent molecule, $\sigma$ is the solvent-accessible surface of the particle, and $\sigma\ \delta$ is the volume of the local domain. According to this model, $\delta$ is directly proportional to the salting-out strength of the additive. Our goal is to show that $n_w/N_w$ is independent of $\delta$.

To obtain an expression for the number of water molecules transported by the particle, $n_w$, we need to consider the relative motion of the solvent molecules parallel to the particle interface. Specifically, we want an expression for the $x$ component of solvent velocity, $u_x(y)$. At the particle surface ($y = 0$), we apply the no-slip boundary condition: $u_x^0 \equiv u_x\ (0) = 0$. As the distance from the particle surface increases within the local domain, the solvent velocity will gradually grow, reaching its bulk value: $u_x^\infty \equiv u_x(\delta)$. The variation of $u_x$ within the local domain of the particle will allow us to obtain $n_w$.

The velocity profile is extracted from the Navier–Stokes equation for incompressible fluids:[20]

$$(\partial p/\partial y) + G_2(x, y)(\mathrm{d}W/\mathrm{d}y) = 0 \tag{5a}$$

$$\eta(\partial^2 u_x/\partial y^2) - (\partial p/\partial x) = 0 \tag{5b}$$

where $p(x,y)$ describes the pressure profile of the fluid and $\eta$ its viscosity. The function $p(x,y)$ is obtained by integrating eq 5a within the domain: $0 \leq y \leq \delta$. Integration starts at $y=\delta$, where $p=p_\infty$ is the hydrostatic pressure, and $W = 0$. The integrated expression, $p = p_\infty + k_BTC_2(x)$, is then inserted in eq 5b, yielding $\partial^2 u_x/\partial y^2 = (k_BT/\eta)(\mathrm{d}C_2/\mathrm{d}x)$. The velocity profile is obtained by performing a first integration with respect to $y$ starting from $y = \delta$, where $\partial u_x/\partial y = 0$. A second integration, which is performed starting from $u_x(0) = 0$, gives $u_x = (k_BT/\eta)(\mathrm{d}C_2/\mathrm{d}x)\ (\delta - y/2)y$, with the bulk value being $u_x^\infty = (k_BT/\eta)(\mathrm{d}C_2/\mathrm{d}x)(\delta^2/2)$. This velocity profile is shown in Figure 4.

The hydration parameter, $n_w$, has been introduced by considering a two-state model for the motion of solvent molecules.[58] Specifically, solvent molecules are assumed to migrate either as bulk solvent ($u_x = u_x^\infty$) or together with the particle ($u_x = u_x^0$). To formulate a correspondence between $n_w$ and $u_x(y)$, which gradually varies from $u_x^0$ to $u_x^\infty$, we calculate the solvent mean velocity within the local domain: $\langle u_x\rangle = \delta^{-1}\int_0^\delta u_x\, dy = (2/3)u_x^\infty$. This quantity can be equivalently describe as the weighted average between the two limiting velocity values, $u_x^0$ and $u_x^\infty$. In other words, within the local domain of the particle, we consider an inner subdomain, in which solvent molecules migrate together with the particle, and an outer subdomain where solvent migration is the same as that in the bulk fluid. If $\delta_u$ is the position of the boundary between these two subdomains (see Figure 4), we have $n_w = \sigma\ \delta_u/v_w$. We find that $\delta_u = (1/3)\delta$ by applying the condition $\langle u_x\rangle\delta = \int_0^{\delta_u} u_x^0 \mathrm{d}y + \int_{\delta_u}^{\delta} u_x^\infty \mathrm{d}y$, and conclude that $n_w/N_w = 1/3$.

This predicted value of $n_w/N_w$ is significantly smaller than our experimental values in Table 2. Clearly, factors such as particle shape, surface roughness, solvation, and other chemical interactions, which are ignored by this model, are expected to play an important role in the actual magnitude of $n_w/N_w$.

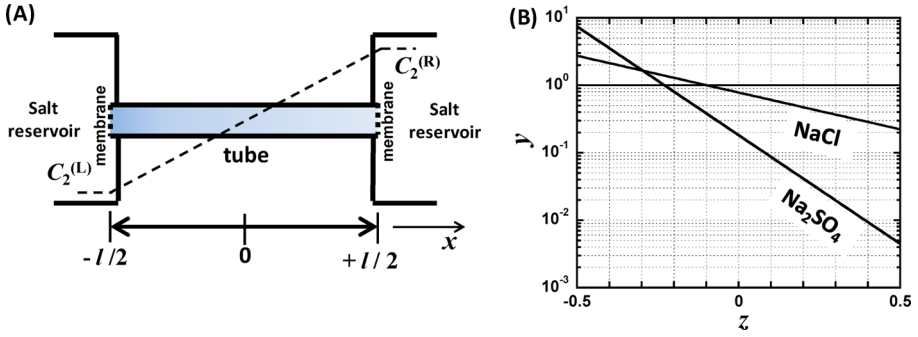


**Figure 5.** (A) Schematic diagram for examining the role of polymer diffusiophoresis in conditions of steady-state diffusion. A tube of length $l$ contains a polymer solution and is connected to two salt reservoirs with salt concentrations $C_2^{(L)}$ and $C_2^{(R)}$. The dashed line with positive slope describes the salt concentration profile, $C_2 = \overline{C}_2 + \Delta C_2(x/l)$ in steady-state conditions, where $\overline{C}_2 \equiv (C_2^{(L)} + C_2^{(R)})/2$ and $\Delta C_2 = C_2^{(R)} - C_2^{(L)}$. The two vertical dashed lines at the tube extremities denote two membranes not permeable to the polymer component. (B) Logarithmic diagram showing three normalized polymer concentration profiles, $y \equiv C_1/C_1^0$ (solid lines), as a function of the normalized position, $z \equiv x/l$, inside the tube obtained for $\beta = 0$ (baseline), $\beta = 2.5$ (NaCl), and $\beta = 7.4$ ($Na_2SO_4$).


dx.doi.org/10.1021/la503214b | Langmuir 2014, 30, 12210−12219

Nonetheless, this simple model provides a theoretical basis for $n_w$ and shows, in agreement with our experimental findings, that $n_w/N_w$ is independent of $\delta$. In other words, $N_w - n_w$ is proportional to the salting-out strength of the additive.

**3.5. Significance of Diffusiophoresis.** Polymer diffusiophoresis from high to low salt concentration increases with salting-out strength. This mechanism may play an important role in mass-transfer processes in which nonuniform salt concentrations occur. In general, numerical simulations are needed to compute solute concentration profiles and assess the significance of cross-diffusion in the investigated process. Nonetheless, there are few examples for which analytical expressions of concentration profiles can be obtained.[27,60] These are valuable because they straightforwardly show the effect of cross-diffusion coefficients on concentration profiles and fluxes. Recently, we have identified a steady-state diffusion process that is appropriate for the theoretical examination of diffusiophoresis of large particles (i.e., macromolecules and nanoparticles) in the presence of gradients of low molecular-weight additives (i.e., salts, osmolytes, ligands, and denaturants). This was examined in order to evaluate the effect of particle size on the relative importance of salt-induced diffusiophoresis compared to the intrinsic Brownian diffusion of the particle.[27] Here, this steady-state diffusion process is examined to evaluate the effect of salting-out strength on particle diffusiophoresis.

We consider steady-state diffusion occurring between two compartments containing binary salt−water solutions at different salt concentrations. As shown in Figure 5A, two large and well-stirred compartments, with constant salt concentrations $C_2^{(L)}$ and $C_2^{(R)}$, are separated by an intermediate section with length, $l$, representing a tube positioned between $x = -l/2$ and $x = +l/2$. The two tube extremities are capped with semipermeable membranes and attached to both compartments. This tube initially contains a uniform polymer solution with concentration, $C_1^0$. If this concentration is sufficiently low, salt osmotic diffusion can be neglected, and polymer diffusion can be approximately described by its tracer-diffusion coefficient.

The net rate of polymer diffusion with respect to the solvent component is given by[27]

$$u_1 = -D_1^0(\nabla \ln C_1 + \nu_2 \hat{D}_{12} \nabla \ln a_2) \quad (6)$$

where $a_2$ is the salt thermodynamic activity. The first term on the right side of eq 6 represents the Brownian entropic driving force, while the second term, which is weighed by $\hat{D}_{12}$, describes the directional chemical field introduced by the gradient of salts or other additives. In steady-state conditions, the condition $u_1 = 0$ must be respected throughout the tube because particles cannot cross the two membranes. Thus, we have $(\mathrm{d} \ln C_1/\mathrm{d}C_2) = -\nu_2 b_{12}$, where we have used $\hat{D} = b_{12} C_2$ and neglected salt thermodynamic nonideality for simplicity. Its integration yields $y = (\beta/2) \exp(-\beta z)/\sinh(\beta/2)$, where $y \equiv C_1/C_1^0$, $z \equiv x/l$, and $\beta \equiv b_{12}\cdot(\nu_2 \Delta C_2)$, with $\Delta C_2 = C_2^{(R)} - C_2^{(L)}$, and we have applied the mass-conservation condition[27] $C_1^0 = l^{-1} \int_{-l/2}^{+l/2} C_1 \mathrm{d}x$. Normalized concentration profiles of polymer, $y(z)$, induced by the osmolar-concentration difference of $\nu_2 \Delta C_2 = 1$ mol·dm$^{-3}$ are illustrated for NaCl ($\beta = 2.5$) and $Na_2SO_4$ ($\beta = 7.4$) in Figure 5B. These two logarithmic profiles show that polymer concentration is enhanced and depleted near the left and right membrane locations, respectively, due to salting-out interactions. In the case of NaCl, the polymer concentration near the left compartment is predicted to be 2.7 times the value of $C_1^0$, while that near the right compartment is predicted to be 22% of $C_1^0$. Similar results are predicted for the other chloride salts. However, in the case of $Na_2SO_4$, diffusiophoretic effects are more dramatic. Specifically, the corresponding enrichment and depletion of polymer are given by $y(-0.5) = 7.4$ and $y(+0.5) = 0.0044$, respectively. We believe that diffusiophoresis of macromolecules induced by strong salting-out agents such as $Na_2SO_4$ are significant and can be exploited in diffusion-based mass-transfer processes. For example, devices based on Figure 5A could be used to design and control the self-assembly and crystallization of macromolecules (e.g., proteins) near a membrane (left membrane in Figure 5A) or facilitate the adsorption of macromolecules on solid supports positioned near this membrane.

## 4. SUMMARY AND CONCLUSIONS

We have characterized the effect of salting-out strength on the magnitude of cross-diffusion coefficients and the related deviation of $D_{DLS}$ from $D_{11}$. Salt osmotic diffusion, $\hat{D}_{12}(C_2)$, is directly related to the preferential-hydration parameter, $N_w$. The extracted values of $N_w$, which characterize the salting-out strength of salts, are in agreement with the anionic and cationic Hofmeister series. PEG diffusiophoresis, $\hat{D}_{12}(C_2)$, was found to be proportional to the salting-out strength of the employed salt. This finding, which is related to $n_w/N_w$ being approximately independent of salt type, was supported by hydrodynamic considerations on $n_w$. Our analysis of a steady-state diffusion problem has shown that gradients of strong salting-out agents such as $Na_2SO_4$ can produce large enhancements and depletions of polymer concentration. Related devices could be exploited to promote the condensation of macromolecules near interfaces.

## ■ ASSOCIATED CONTENT

### Supporting Information

Tables reporting ternary diffusion coefficients in the volume- and solvent-fixed reference frames of the investigated ternary systems, related volumetric properties, thermodynamic and transport parameters of the binary salt-water systems, and DLS diffusion coefficients are provided as Supporting Information. This material is available free of charge via the Internet at http://pubs.acs.org/.

## ■ AUTHOR INFORMATION


### Corresponding Author

*Mailing address: Department of Chemistry, Box 298860, Texas Christian University, Fort Worth, Texas 76129, USA. Phone: (817) 257-6215. Fax: (817) 257-5851. E-mail: O.Annunziata@tcu.edu.

### Present Address

‡Alcon Research Ltd., Fort Worth, Texas 76134.

### Author Contributions

†These two authors equally contributed to this work.


### Notes

The authors declare no competing financial interest.

## ■ ACKNOWLEDGMENTS

This work was supported by the ACS Petroleum Research Fund (47244-G4) and TCU Research and Creative Activity Funds.

## REFERENCES


(1) Bird, R. B. Five decades of transport phenomena. *AIChE J.* **2003**, *50*, 273−287.
(2) Curtiss, C. F.; Bird, R. B. Multicomponent diffusion. *Ind. Eng. Chem. Res.* **1999**, *38*, 2515−2522.
(3) Tyrrell, H. J. V.; Harris, K. R. *Diffusion in Liquids*; Butterworths: London, 1984.
(4) Keurentjes, J. T. F.; Janssena, A. E. M.; Broeka, A. P.; Van der Padta, A.; Wesselingh, J. A.; Van't Riet, K. Multicomponent diffusion in dialysis membranes. *Chem. Eng. Sci.* **1992**, *47*, 1963−1971.
(5) Petsev, D. N.; Chen, K.; Gliko, O.; Vekilov, P. G. Diffusion-limited kinetics of the solution-solid phase transition of molecular substances. *Proc. Natl. Acad. Sci. U.S.A.* **2003**, *100*, 792−796.
(6) Gedik, E. T. Surface Chemistry in SPR Technology. In *Handbook of Surface Plasmon Resonance*; Schasfoort, R. B. M.; Tudos, A. J., Eds.; Royal Chemical Society: Cambridge, 2008; pp 173−220.
(7) Kanjickal, D. G.; Lopina, S. T. Modeling of drug release from polymeric delivery systems. *Crit. Rev. Ther. Drug Carrier Syst.* **2004**, *21*, 345−386.
(8) Brackley, C. A.; Cates, M. E.; Marenduzzo, D. Intracellular Facilitated Diffusion: Searchers, Crowders, and Blockers. *Phys. Rev. Lett.* **2013**, *111*, 108101.
(9) Miguez, D. G.; Vanag, V. K.; Epstein, I. R. Fronts and pulses in an enzymatic reaction catalyzed by glucose oxidase. *Proc. Natl. Acad. Sci. U.S.A.* **2007**, *104*, 6992−6997.
(10) Vanag, V. K.; Epstein, I. R. Cross-diffusion and pattern formation in reaction-diffusion systems. *Phys. Chem. Chem. Phys.* **2009**, *11*, 897−912.
(11) Garcia-Ruiz, J. M. Counterdiffusion methods for macromolecular crystallization. *Meth. Enzym.* **2003**, *368*, 130−154.
(12) Lin, C. C.; Anseth, K. S. PEG hydrogels for the controlled release of biomolecules in regenerative medicine. *Pharm. Res.* **2009**, *26*, 631−643.
(13) Whitesides, G.M. The origin and the future of microfluidics. *Nature* **2006**, *442*, 368−373.
(14) Weigl, B. H.; Yager, P. Microfluidics: Microfluidic diffusion-based separation and detection. *Science* **1999**, *283*, 346−347.
(15) Atencia, J.; Beebe, D. J. Controlled microfluidic interfaces. *Nature* **2005**, *437*, 648−655.
(16) Jervais, T.; Jensen, K. F. Mass transport and surface reactions in microfluidic systems. *Chem. Eng. Sci.* **2006**, *61*, 1102−1121.
(17) Dror, I.; Amitay, T.; Yaron, B.; Berkowitz, B. Salt-pump mechanism for contaminant intrusion into coastal aquifers. *Science* **2003**, *300*, 950.
(18) Schurr, J. M.; Fujimoto, B. S.; Huynh, L.; Chiu, D. T. A theory of macromolecular chemotaxis. *J. Phys. Chem. B* **2013**, *117*, 7626−7652.
(19) Keh, H. J.; Anderson, J. L. Colloid transport by interfacial forces. *Annu. Rev. Fluid Mech.* **1989**, *21*, 61−99.
(20) Schaeiwitz, J. A.; Lechnick, W. J. Ternary diffusion formulation for diffusiophoresis. *Chem. Eng. Sci.* **1984**, *39*, 799−807.
(21) Abécassis, B.; Cottin-Bizonne, C.; Ybert, C.; Ajdari, A.; Bocquet, L. Boosting migration of large particles by solute contrasts. *Nat. Mater.* **2008**, *7*, 785−789.
(22) Palacci, J.; Abécassis, B.; Cottin-Bizonne, C.; Ybert, C.; Bocquet, L. Colloidal motility and pattern formation under rectified diffusiophoresis. *Phys. Rev. Lett.* **2010**, *104*, 138302.
(23) Abécassis, B.; Cottin-Bizonne, C.; Ybert, C.; Ajdari, A.; Bocquet, L. Osmotic manipulation of particles for microfluidic applications. *New J. Phys.* **2009**, *11*, 075022.
(24) Florea, D.; Sami Musaa, S.; Huyghea, J. M. R.; Wyss, H. M. Long-range repulsion of colloids driven by ion exchange and diffusiophoresis. *Proc. Natl. Acad. Sci. U.S.A.* **2014**, *111*, 6554−6559.
(25) Prieve, D. C. Migration of a colloidal particle in a gradient of electrolyte concentration. *Adv. Coll. Interface Sci.* **1982**, *16*, 321−335.
(26) Annunziata, O.; Buzatu, D.; Albright, J. G. Protein diffusiophoresis and salt osmotic diffusion in aqueous solutions. *J. Phys. Chem. B* **2012**, *116*, 12694−12705.
(27) McAfee, M. S.; Annunziata, O. Effect of particle size on salt-induced diffusiophoresis compared to brownian mobility. *Langmuir* **2012**, *30*, 4916−4923.
(28) Arakawa, T.; Timasheff, S. N. Preferential interactions of proteins with salts in concentrated solutions. *Biochemistry* **1982**, *21*, 6545−6552.
(29) Record, M. T.; Anderson, C. F. Interpretation of preferential interaction coefficients of nonelectrolytes and of electrolyte ions in terms of a two domain model. *Biophys. J.* **1995**, *68*, 786−794.
(30) Albertsson, P. A. *Partition of Cell Particles and Macromolecules*; Wiley: New York, 1986.
(31) McPherson, A. *Crystallization of Biological Macromolecules*; Cold Spring Harbor: New York, 1998.
(32) Tan, C.; Albright, J. G.; Annunziata, O. Determination of preferential-interaction parameters by multicomponent diffusion. Applications to the poly(ethylene glycol)−salt−water ternary mixtures. *J. Phys. Chem. B* **2008**, *112*, 4967−4974.
(33) Collins, K. D.; Washabaugh, M. W. The Hofmeister effect and the behaviour of water at interfaces. *Q. Rev. Biophys.* **1985**, *18*, 323−422.
(34) Cacace, M. G.; Landau, E. M.; Ramsden, J. J. The Hofmeister series: salt and solvent effects on interfacial phenomena. *Q. Rev. Biophys.* **1997**, *30*, 241−277.
(35) Zhang, Y. J.; Furyk, S.; Sagle, L. B.; Cho, Y.; Bergbreiter, D. E.; Cremer, P. S. Effects of Hofmeister Anions on the LCST of PNIPAM as a Function of Molecular Weight. *J. Phys. Chem. C* **2007**, *111*, 8916−8924.
(36) Okur, H. I.; Kherb, J.; Cremer, P. S. Cations Bind Only Weakly to Amides in Aqueous Solutions. *J. Am. Chem. Soc.* **2013**, *135*, 5062−5067.
(37) Zhang, Y. J.; Cremer, P. S. Interactions between macromolecules and ions: The Hofmeister series. *Curr. Opin. Chem. Biol.* **2006**, *10*, 658−663.
(38) Zhang, Y. J.; Cremer, P. S. Chemistry of Hofmeister anions and osmolytes. *Annu. Rev. Phys. Chem.* **2010**, *61*, 63−83.
(39) Annunziata, O.; Buzatu, D.; Albright, J. G. Protein Diffusion coefficients determined by Macroscopic-Gradient Rayleigh Interferometry and Dynamic Light Scattering. *Langmuir* **2005**, *21*, 12085−12089.
(40) Schmitz, K. S. *Introduction to Dynamic Light Scattering by Macromolecules*; Academic Press: San Diego, CA, 1990.
(41) Sutherland, E.; Mercer, S. M.; Everist, M.; Leaist, D. G. Diffusion in solutions of micelles. What does dynamic light scattering measure? *J. Chem. Eng. Data* **2009**, *54*, 272−278.
(42) Miller, D. G.; Rard, J. A. Mutual diffusion coefficients of $BaCl_2$−$H_2O$ and KCl−$H_2O$ at 25 °C from Rayleigh interferometry. *J. Chem. Eng. Data* **1980**, *25*, 211−215.
(43) Rard, J. A. Isopiestic determination of the osmotic coefficients of $Lu_2(SO_4)_3$(aq) and $H_2SO_4$(aq) at the temperature $T$ = 298.15 K, and review and revision of the thermodynamic properties of $Lu_2(SO_4)_3$(aq) and $Lu_2(SO_4)_3{\cdot}8H_2O$(cr). *J. Chem. Thermodyn.* **1996**, *28*, 83−110.
(44) Rard, J. A.; Miller, D. G. The mutual diffusion coefficients of NaCl−$H_2O$ and $CaCl_2$−$H_2O$ at 25 °C from Rayleigh interferometry. *J. Sol. Chem.* **1979**, *8*, 701−716.
(45) Rard, J. A.; Miller, D. G. The mutual diffusion coefficients of $Na_2SO_4$−$H_2O$ and $MgSO_4$−$H_2O$ at 25 °C from Rayleigh interferometry. *J. Sol. Chem.* **1979**, *8*, 755−766.
(46) Rard, J. A.; Clegg, S. L.; Palmer, D. A. Isopiestic determination of the osmotic coefficients of $Na_2SO_4$(aq) at 25 and 50 °C, and representation with ion-interaction (Pitzer) and mole fraction thermodynamic models. *J. Sol. Chem.* **2000**, *29*, 1−49.
(47) Miller, D. G.; Albright, J. G. Optical methods. In *Measurement of the Transport Properties of Fluids: Experimental Thermodynamics*, Vol. *III*; Wakeham, W. A., Nagashima, A., Sengers, J.V., Eds.; Blackwell Scientific Publications: Oxford, 1991; pp 272−294.
(48) Miller, D. G.; Vitagliano, V.; Sartorio, R. Some comments on multicomponent diffusion: Negative main term diffusion coefficients,

second law constraints, solvent choices, and reference frame transformations. *J. Phys. Chem.* **1986**, *90*, 1509−1519.
(49) Miller, D. G. A method for obtaining multicomponent diffusion coefficients directly from rayleigh and gouy fringe position data. *J. Phys. Chem.* **1988**, *92*, 4222−4226.
(50) Zhang, H.; Annunziata, O. Effect of macromolecular polydispersity on diffusion coefficients measured by Rayleigh interferometry. *J. Phys. Chem. B* **2008**, *112*, 3633−3643.
(51) Lomakin, A.; Teplow, D. B.; Benedek, G. B. In *Methods in Molecular Biology Amyloid Proteins: Methods and Protocols*; Sigurdsson, E. M., Ed.; Humana Press: Totowa, NJ, 2005; Vol. *299*, pp153−174.
(52) Tanford, C. *Physical Chemistry of Macromolecules*; Wiley: New York, 1961; p 356.
(53) Zhang, H.-L.; Han, S.-J. Viscosity and Density of Water + Sodium Chloride + Potassium Chloride Solutions at 298.15K. *J. Chem. Eng. Data* **1996**, *41*, 516−520.
(54) Lobo, V. M. M.; Quaresma, J. L. *Handbook of Electrolyte Solutions*; Elsevier: Amsterdam, 1989.
(55) Isono, T. Density, viscosity, and electrolytic conductivity of concentrated aqueous electrolyte solutions at several temperatures. Alkaline-earth chlorides, lanthanum chloride, sodium chloride, sodium nitrate, sodium bromide, potassium nitrate, potassium bromide, and cadmium nitrate. *J. Chem. Eng. Data* **1984**, *29*, 45−52.
(56) Vergara, A.; Paduano, L.; Vitagliano, V.; Sartorio, R. Mutual diffusion in aqueous solution of poly(ethylene glycol) samples. Some comments on the effect of chain length and polydispersity. *Phys. Chem. Chem. Phys.* **1999**, *1*, 5377−5383.
(57) Brown, W. Slow-Mode Diffusion in Semidilute Solutions Examined by Dynamic Light Scattering. *Macromolecules* **1984**, *17*, 66−72.
(58) Annunziata, O. On the role of solute solvation and excluded-volume interactions in coupled diffusion. *J. Phys. Chem. B* **2008**, *112*, 11968−11975.
(59) Annunziata, O.; Payne, A.; Wang, Y. Solubility of lysozyme in the presence of aqueous chloride salts: common-ion effect and its role on solubility and crystal thermodynamics. *J. Am. Chem. Soc.* **2008**, *130*, 13347−13352.
(60) Zhang, H.; Annunziata, O. Modulation of drug transport properties by multicomponent diffusion in surfactant aqueous solutions. *Langmuir* **2008**, *24*, 10680−10687.